A&A 543, A157 (2012)
DOI: 10.1051/0004-6361/201118560

Astronomy & Astrophysics

Hyperons in neutron-star cores and a 2 $M_\odot$ pulsar

I. Bednarek[2], P. Haensel[1], J. L. Zdunik[1], M. Bejger[1], and R. Mańka[2,⋆]

[1] N. Copernicus Astronomical Center, Polish Academy of Sciences, Bartycka 18, 00-716 Warszawa, Poland
e-mail: ilona.bednarek@us.edu.pl,[bejger;haensel;jlz]@camk.edu.pl
[2] Department of Astrophysics and Cosmology, Institute of Physics, University of Silesia, Uniwersytecka 4, 40-007 Katowice, Poland

Received 1 December 2011 / Accepted 16 April 2012

ABSTRACT

Context. A recent measurement of the mass of PSR J1614-2230 rules out most existing models of the equation of state (EOS) of dense matter that is subjected to the high-density softening caused by either hyperonization or a phase transition to either quark matter or a boson condensate.

Aims. We attempt to resolve the apparent differences between the predictions derived from up-to-date hypernuclear data, which include the appearance of hyperons at about three nuclear densities and the existence of a $M = 2.0\ M_\odot$ neutron star.

Methods. We consider a non-linear relativistic mean field (RMF) model involving the baryon octet coupled to meson fields. An effective Lagrangian includes quartic terms in the meson fields. The values of the model parameters are obtained by fitting the semi-empirical parameters of nuclear matter at the saturation point, as well as potential wells for hyperons in nuclear matter and the strength of the $\Lambda - \Lambda$ attraction in double-Λ hypernuclei.

Results. We propose a non-linear RMF model that is consistent with up-to-date semi-empirical nuclear and hypernuclear data and allows for neutron stars with hyperon cores and $M > 2\ M_\odot$. The model involves hidden-strangeness scalar and vector mesons, coupled only to hyperons, and quartic terms involving vector meson fields.

Conclusions. Our EOS involving hyperons is stiffer than the corresponding nucleonic EOS (in which hyperons are artificially suppressed) above five nuclear densities. The required stiffening is generated by the quartic terms involving the hidden-strangeness vector meson.

Key words. dense matter – equation of state – stars: neutron

1. Introduction

A recent measurement of the mass of PSR J1614-2230, $1.97 \pm 0.04\ M_\odot$ (Demorest et al. 2010), puts a stringent constraint on the equation of state (EOS) of dense matter in neutron star cores. In the light of this measurement, EOSs of dense matter, which are based on the modern many-body theories and the realistic strong-interaction model, lead to a puzzle. On the one hand, interactions consistent with the available experimental data on hypernuclei, predict the presence of hyperons at densities exceeding $2{-}3\rho_0$, where $\rho_0 = 2.7 \times 10^{14}$ g cm^{-3} (corresponding to the baryon number density $n_0 = 0.16$ fm^{-3}) is the normal nuclear density. On the other hand, the inevitable softening of the EOS, due to the hyperonization, implies that the maximum allowable mass is $M_{\rm max} \lesssim 1.5\ M_\odot$ (see, e.g. Burgio et al. 2011; Vidana et al. 2011, and references therein). Such a low value of $M_{\rm max}$ is only marginally consistent with that of $1.44\ M_\odot$ measured for the Hulse-Taylor pulsar, but has been placed in doubt by that of $1.67 \pm 0.04\ M_\odot$ for PSR J1903-0327 (Champion et al. 2008; a more precise value was obtained by Freire et al. 2011). Vidana et al. (2011) noted that this problem cannot be solved by adding an ad hoc extremely stiff repulsive three-body contribution to the EOS.

We consider neutron star cores composed of baryons, electrons, and muons. Baryons and leptons are in weak-interaction equilibrium. Hyperons appear at density ρ_1 (baryon density n_1). For $\rho < \rho_1$, only nucleons are present. For $\rho > \rho_1$, matter contains a mixture of nucleons and hyperons. This state (phase) is denoted NH. We also consider a "reference dense-matter model" with hyperons artificially suppressed. This purely nucleon state is denoted N. The corresponding EOSs are denoted EOS.NH and EOS.N. These EOSs coincide for $\rho < \rho_1$.

A too low $M^{\rm (NH)}_{\rm max}$ is not an inevitable feature of neutron stars with hyperon cores. Bonanno & Sedrakian (2012) obtained $M^{\rm (NH)}_{\rm max} > 2\ M_\odot$, starting from an extremely stiff relativistic mean field model NL3 EOS.N, which yielded $M^{\rm (N)}_{\rm max} = 2.8\ M_\odot$ (close to the absolute upper bound on $M_{\rm max}$ stemming from causality, e.g., Haensel et al. 2007). Bonanno & Sedrakian (2012) extend the NL3 model to the hyperon sector, and get $M^{\rm (NH)}_{\rm max} = 2.03\ M_\odot$. Massive stars with hyperon cores exist there because of the extreme stiffness of the EOS.N, and the nuclear-matter parameter (the slope of symmetry energy versus density) $L = 118$ MeV is significantly higher than its semi-empirical estimates.

In our approach, we keep L (and the stiffness of the EOS.N near ρ_0) within the semi-empirical estimates (i.e., those obtained within a model of atomic nuclei, hence model-dependent values). Our EOS.N at high density is stiff, but not extremely stiff: $M^{\rm (N)}_{\rm max} = 2.1\ M_\odot$. In general, $M^{\rm (NH)}_{\rm max}$ is essentially determined by the $\rho \gtrsim 5\rho_0$ segment of the EOS.NH. Hence if the hyperon softening occurs at $2{-}3\rho_0$, then, to get a sufficiently high $M_{\rm max}$, the softening must be followed by a sufficiently strong *stiffening* of EOS.NH for $\rho \gtrsim 5\rho_0$. One has therefore to identify a mechanism that stiffens the EOS.NH at these densities. For our model of EOS.N, in order to yield $M^{\rm (NH)}_{\rm max} > 2\ M_\odot$, the EOS.NH for $\rho \gtrsim 5\rho_0$ should be actually *stiffer* than the EOS.N one. Simultaneously, the NH phase has to be stable (thermodynamically preferred over

⋆ Retired.

the N one). We derive a constraint on the EOS.NH resulting from the conditions mentioned above, and discuss the consequences of the violation of this constraint.

In our discussion, we restrict ourselves to hadronic matter, and do not consider the possibility of quark deconfinement. Because of the surface effects and electrical screening in a quark plasma, a transition to quark matter would occur at nearly constant pressure and with an only slightly smoothed density jump (see, e.g., Endo et al. 2006, and references therein). A reasonable scenario is: softening of the N phase by hyperonization at 2–3ρ_0, followed by softening of the NH phase by quark deconfinement at a significantly higher density. Bonanno & Sedrakian (2012) show that assuming NL3 EOS.NH, a transition to quark matter occurring after hyperonization could be consistent with the detection of 2 $M_\odot$ neutron star provided that the vector repulsion in quark matter is sufficiently strong and quark deconfinement takes place near the maximum NS mass. For our EOS.NH, getting 2 $M_\odot$ with a quark core would require a very fine tuning, and we do not consider such an unlikely possibility.

The problem of an interplay between attraction (softening) and repulsion (stiffening) in dense hadronic matter can be formulated in simple terms using a modern effective field theory, involving baryon and meson fields. In the case of nucleon matter, such a theory can be put on a firm theoretical basis, starting from quantum chromodynamics (QCD) (Walecka 2004, and references therein). Such an effective theory can be solvable within the mean field approximation and can give a satisfactory description of a wealth of nuclear physics data if the coupling of nucleons to the scalar meson field σ, and two vector meson fields: ω_μ and ρ^i_μ, is considered. Here, μ and i denote the space-time and isospin-space components of the field. An effective Lagrangian contains quadratic and quartic terms in vector fields, and quadratic, cubic, and quartic terms in scalar fields. While σ yields an attraction to bind nuclei, vector meson fields generate repulsion to saturate nuclear matter at ρ_0. Numerical coefficients in the effective Lagrangian are fixed by fitting a wealth of nuclear data (Sugahara & Toki 1994). The effective model is then extended to include the hyperon sector. Two meson fields with “hidden strangeness” ($\bar{s}s$) are added: scalar σ^* (quadratic terms) and vector-isovector ϕ^i_μ (quadratic and quartic terms). These fields couple only to hyperons (Schaffner et al. 1994). An important constraint on the hyperon sector of Lagrangian results from the existing evaluations of the depth of the potential well acting on a single zero-momentum hyperon in nuclear matter, $U^{(N)}_\Lambda$, $U^{(N)}_\Sigma$, and $U^{(N)}_\Xi$ (binding energy of a hyperon in nuclear matter is $B_\mathrm{H} = -U^{(N)}_\mathrm{H}$). An effective theory of hadronic matter described in the general terms above and solved in the mean field approximation are referred to as a non-linear relativistic mean field model (non-linear RMF, Bednarek & Mańka 2009).

There exist a few older and simpler models of NH matter that predict that $M^{(\mathrm{NH})}_\mathrm{max} > 2\ M_\odot$. These models are based on the relativistic mean field Lagrangian involving an octet of baryons coupled to the σ, ω_μ, and ρ^i_μ meson fields (quadratic terms in the Lagrangian), with additional cubic and quartic σ self-interaction terms (for a review, see Glendenning 1996). The mean field solutions of the field equations are referred to collectively as the relativistic mean field (RMF) model. Glendenning & Moszkowski (1991) can exceed 2 $M_\odot$ assuming high nuclear matter incompressibility, K = 300 MeV, and a strong $\Lambda - \sigma$ attraction, balanced by a $\Lambda - \omega$ repulsion to be consistent with an experimental $U^{(N)}_\Lambda$. Experimental constraints on U_Σ and U_Ξ in nuclear matter are not applied. It is assumed that all hyperons in the baryon octet have the same coupling as Λ.

A model similar to that of Glendenning & Moszkowski (1991) was used to obtain $M^{(\mathrm{NH})}_\mathrm{max} > 2\ M_\odot$ by Bombaci et al. (2008). Dexheimer & Schramm (2008) applied a hadronic chiral model of NH matter. They treated mesons and the baryon octet as flavor-SU(3) multiplets. For one form of the quartic term in the vector-meson fields, they obtained $M^{(\mathrm{NH})}_\mathrm{max} = 2.06\ M_\odot$.

Two specific ways of ensuring that $M^{(\mathrm{NH})}_\mathrm{max} > 2\ M_\odot$ have been proposed. The first way, chosen in both our work and Weissenborn et al. (2012b,a), consists in introducing a hyperon repulsion due to a hidden-strangeness vector meson ϕ_μ that couples only to hyperons. The second way, pointed out in Weissenborn et al. (2012a), consists in making vector-meson – hyperon repulsion stronger by going from the SU(6) symmetry relations to the SU(3) ones. In contrast to Weissenborn et al. (2012a), we keep the vector-meson – hyperon coupling constants at their SU(6) values.

In the present paper, we propose a resolution to the problem of the “hyperonization – $M_\mathrm{max} > 2\ M_\odot$” using a specific realization of the non-linear RMF model of hadronic matter (Bednarek & Mańka 2009). The non-linear RMF model of NH matter is presented in Sect. 2. Experimental constraints from nuclear and hypernuclear physics are described in Sect. 3. A particular EOS.NH is described in Sect. 4. A model of PSR J1614-2230 with a hyperon core is presented in Sect. 5. The problem of the high-density instability of the NH phase and the $M - R$ relation for neutron stars models are discussed in Sect. 6. Finally, in Sect. 7 we summarize the results of the paper, compare them with results obtained by other authors, and present our conclusions.

Preliminary results of our work were presented at the MODE-SNR-PWN Workshop in Bordeaux, France, November 15–17, 2010, and in a poster at the CompStar 2011 Workshop in Catania, Italy, May 9–12, 2011.

2. Non-linear RMF model of hyperon cores

Our adopted model was formulated by Bednarek & Mańka (2009). The octet of baryons includes a nucleon doublet N and six of the lowest-mass hyperons H: Λ singlet, Σ triplet, and Ξ doublet. The uniform number density of each baryon species B is denoted n_B ($B = n, p, \Lambda, \ldots$).

In the nucleon sector, the meson fields are: scalar σ, vector ω_μ, and vector-isovector ρ^i_μ. The generalization of the non-linear RMF model to the baryon octet is done in the following way. Additional “hidden-strangeness” mesons, namely scalar $\sigma^\star$ and vector ϕ_μ, are introduced. They couple only to hyperons, such that $g_{N\sigma^\star} = g_{N\phi} = 0$. The vector-meson coupling constants to hyperons are assumed to fulfill the relations stemming from the SU(6) symmetry (additive quark model) of hadrons

$$
\begin{aligned}
g_{\Lambda\omega} &= g_{\Sigma\omega} = 2g_{\Xi\omega} = \frac{2}{3}g_{N\omega}, \\
g_{\Lambda\rho} &= 0,\ g_{\Sigma\rho} = 2g_{\Xi\rho} = 2g_{N\rho}, \\
g_{N\phi} &= 0,\ g_{\Lambda\phi} = g_{\Sigma\phi} = \frac{g_{\Xi\phi}}{2} = -\frac{\sqrt{2}}{3}g_{N\omega}.
\end{aligned}
\tag{1}
$$

Similar symmetry relations can be obtained for the coupling constants of the scalar mesons, but they are not used in the present model. We instead adjust them to fit experimental estimates of $U^{(N)}_B$.

At fixed $\{n_B\}$ ($B = n, p, \Lambda, \ldots$), and assuming vanishing baryon currents, the hadronic Lagrangian density $\mathcal{L}_\mathrm{had}$ is used to derive the equations of motion for the meson fields. Static solutions are found assuming that baryonic matter is isotropic and uniform. The mean-field approximation, neglecting quantum corrections, is used: $\sigma \longrightarrow \langle\sigma\rangle = s_0$, $\omega_\mu \longrightarrow \langle\omega_\mu\rangle = w_0\delta_{\mu 0}$, $\rho^i_\mu \longrightarrow \langle\rho^i_\mu\rangle = r_0\delta_{\mu 0}\delta_{i3}$, $\sigma^\star \longrightarrow \langle\sigma^\star\rangle = s^\star_0$, $\phi_\mu \longrightarrow \langle\phi_\mu\rangle = f_0\delta_{\mu 0}$. The resulting Lagrangian density function $\mathcal{L}_{\rm had}$ consists of three components, $\mathcal{L}_{\rm had} = \mathcal{L}_{\rm B} + \mathcal{L}^{(2)}_{\rm M} + \mathcal{L}^{(3,4)}_{\rm M}$. The component $\mathcal{L}_{\rm B}$ is obtained from the free-baryon Lagrangian by replacing bare baryon masses m_B ($B = n, p, \Lambda, \ldots$) by the effective ones, $m^\star_B = m_B - g_{B\sigma}s_0 - g_{B\sigma^\star}s^\star_0$. The quadratic (interaction) component $\mathcal{L}^{(2)}_{\rm M}$ contains terms proportional to s_0^2, w_0^2, r_0^2, $s_0^{\star 2}$, and f_0^2. The interaction component $\mathcal{L}^{(3,4)}_{\rm M}$ contains cubic and quartic terms in s_0, and quartic vector-meson terms proportional to w_0^4, r_0^4, and f_0^4 and the cross terms proportional to $f_0^2 w_0^2$, $f_0^2 r_0^2$, and $w_0^2 r_0^2$.

The hadronic Lagrangian density function $\mathcal{L}_{\rm had}$ is then used to calculate the hadron energy-density as a function of partial baryon densities $\{n_B\}$, $\mathcal{E}_{\rm had}(\{n_B\})$. To simplify the formulae, we use the units in which $\hbar = c = 1$, except where indicated otherwise. Calculations done for the considered model (Bednarek & Mańka 2009) lead to the following explicit formulae for the hadron contribution to the energy density $\mathcal{E}$ and pressure P (we note that the original equations of Bednarek & Mańka contain several misprints that are corrected below; for the sake of simplicity, we use a shorthand notation $g_{N\sigma} \equiv g_\sigma, g_{N\omega} \equiv g_\omega, \ldots$)

$$\begin{aligned}\mathcal{E}_{\rm had} &= +\frac{1}{2}m_\sigma^2 s_0^2 + \frac{1}{2}m_\omega^2 w_0^2 + \frac{1}{2}m_\rho^2 r_0^2 + U(s_0)\\ &+ \sum_B \frac{2}{\pi^2}\int_0^{k_{F,B}} k^2 {\rm d}k \sqrt{k^2 + \left(m_B - g_{B\sigma}s_0 \boxed{-g_{B\sigma^\star}s^\star_0}\right)^2}\\ &+3\Lambda_{\rm V}(g_\rho g_\omega)^2 w_0^2 r_0^2 + \frac{3}{4}c_3\left(w_0^4 + r_0^4\right)\\ &\boxed{+\frac{1}{2}m_\phi^2 f_0^2 + \frac{1}{2}m_{\sigma^\star}^2 s_0^{\star 2}} + \boxed{3\left(\frac{1}{8}c_3 + \frac{1}{4}\Lambda_{\rm V}(g_\rho g_\omega)^2\right) f_0^4}\\ &\boxed{+3\left(\frac{3}{4}c_3 - \frac{1}{2}\Lambda_{\rm V}(g_\rho g_\omega)^2\right) f_0^2\left(w_0^2 + r_0^2\right)},\end{aligned} \tag{2}$$

$$\begin{aligned}P_{\rm had} &= -\frac{1}{2}m_\sigma^2 s_0^2 + \frac{1}{2}m_\rho r_0^2 + \frac{1}{2}m_\omega w_0^2 - U(s_0)\\ &+ \sum_B \frac{1}{3\pi^2}\int_0^{k_{F,B}} \frac{k^4 {\rm d}k}{\sqrt{k^2 + \left(m_B - g_{B\sigma}s_0 \boxed{-g_{B\sigma^\star}s^\star_0}\right)^2}}\\ &+\frac{1}{4}c_3(w_0^4 + r_0^4) + \Lambda_{\rm V}(g_\rho g_\omega)^2 w_0^2 r_0^2\\ &\boxed{+\frac{1}{2}m_\phi^2 f_0^2 - \frac{1}{2}m_{\sigma^\star}^2 s_0^{\star 2}} + \boxed{\left(\frac{1}{8}c_3 + \frac{1}{4}\Lambda_{\rm V}(g_\rho g_\omega)^2\right) f_0^4}\\ &\boxed{+\left(\frac{3}{4}c_3 - \frac{1}{2}\Lambda_{\rm V}(g_\rho g_\omega)^2\right) f_0^2(w_0^2 + r_0^2)},\end{aligned} \tag{3}$$

where the non-linear σ-self-interaction potential is

$$U(\sigma) = \frac{1}{3}g_3\sigma^3 + \frac{1}{4}g_4\sigma^4. \tag{4}$$

The terms vanishing in purely nucleon (zero strangeness) matter are presented above in rectangles.

The quartic terms in $\mathcal{E}_{\rm had}$ and $P_{\rm had}$ deserve additional explanations. Their form stems from the chiral SU(3) symmetry of the baryon-meson and meson-meson interactions. The coefficients of the quartic terms involve two phenomenological parameters, c_3 and $\Lambda_{\rm V}$.

We first consider the quartic terms in the nucleon sector. The vector-isoscalar quartic term (w_0^4) was included in the TM1 model of Sugahara & Toki (1994). However, the TM1 model was constructed to describe atomic nuclei, hence is valid for both nuclear matter near saturation density and a small neutron excess. It is to be expected that extrapolation to supranuclear density and large neutron excess would necessitate a richer isospin and density dependence of the model Lagrangian than assumed in the TM1 model. Bednarek & Mańka (2009) proposed to do this by enlarging the quartic terms by adding a vector-isovector one (r_0^4) and a cross-term ($w_0^2 r_0^2$). The strengths of the quartic terms are determined by two parameters, $\Lambda_{\rm V}$ and c_3, instead of only one in the TM1 model of Sugahara & Toki (1994). This allows a good fitting of not only (semi-empirical estimates of) nuclear symmetry energy and incompressibility, but also the slope parameter L, and simultaneously yields $M_{\rm max} > 1.97\,M_{\odot}$.

As shown in Bednarek & Mańka (2009), the chiral SU(3) symmetry yields a suitable extension of the quartic terms to the hyperon sector, the same c_3 and $\Lambda_{\rm V}$ entering the quartic-terms coefficients. Additional quartic terms in the hyperon sector are generated by the hidden-strangeness vector-isoscalar field f_0.

3. Determination of parameters of non-linear RMF model

We denote the neutron excess in nuclear matter by $\delta = (n_n - n_p)/n_{\rm b}$. The energy per nucleon (excluding the nucleon rest energy) is $E(n_{\rm b}, \delta)$. An analysis of a wealth of data on heavy atomic nuclei can yield the parameters of nuclear matter near the saturation point, corresponding to the minimum of energy per nucleon, $E_{\rm s}$, reached at $n_{\rm b} = n_{\rm s}$ and $\delta = 0$. The results are model-dependent and therefore they are called semi-empirical. Other semi-empirical parameters are: the symmetry energy $S_{\rm s}$, the incompressibility $K_{\rm s}$, and the symmetry-energy slope parameter L,

$$\begin{aligned}S_{\rm s} &= \left(\frac{\partial^2 E}{\partial\delta^2}\right)_{n_{\rm s},\delta=0}, \quad K_{\rm s} = 9n_{\rm s}^2\left(\frac{\partial^2 E}{\partial n_{\rm b}^2}\right)_{n_{\rm s},\delta=0},\\ L &= 3n_{\rm s}\left(\frac{\partial^3 E}{\partial n_{\rm b}\partial\delta^2}\right)_{n_{\rm s},\delta=0}.\end{aligned} \tag{5}$$

Studies of hypernuclei and of Σ^- atoms allow us to evaluate the potential energy of a *single* zero-momentum hyperon in symmetric nuclear matter, $U^{(N)}_{\rm H}$. The non-linear RMF yields following expression for this quantity:

$$U^{(N)}_{\rm H} = g_{{\rm H}\sigma}s_0 - g_{{\rm H}\omega}w_0, \tag{6}$$

which should be calculated at $n_{\rm s}$ and $\delta = 0$. The semi-empirical estimates are $U^{(N)}_{\Lambda} = -28$ MeV, $U^{(N)}_{\Sigma} = +30$ MeV, and $U^{(N)}_{\Xi} = -18$ MeV (Schaffner-Bielich & Gal 2000). Equation (6) is then used to determine $g_{\Lambda\sigma}$, $g_{\Sigma\sigma}$, and $g_{\Xi\sigma}$.

As we consider the NH phase, which contains *finite* fractions of hyperons, we need information on the hyperon-hyperon interaction. Studies of double-Λ hypernuclei suggest that the $\Lambda - \Lambda$ interaction is attractive. In the mean-field approximation, it can be characterized by the potential well of a zero-momentum Λ in Λ-matter. In our model we get a general expression for the potential energy of a zero-momentum hyperon H' in H-matter

$$U^{(H')}_{\rm H} = g_{{\rm H}\sigma}s_0 - g_{{\rm H}\omega}w_0 + g_{{\rm H}\sigma^\star}s^\star_0 - g_{{\rm H}\phi}f_0. \tag{7}$$

The latest (very uncertain) semi-empirical estimate coming from double-Λ hypernuclei is $U_\Lambda^{(\Lambda)} = -5$ MeV (Takahashi et al. 2001; Song et al. 2003). Equation (7) is then used to determine $g_{\Lambda\sigma^\star}$. For $U_\Sigma^{(\Sigma)}$ and $U_\Xi^{(\Xi)}$, no data exist. We therefore estimate them using the relations

$$U_\Xi^{(\Xi)} \simeq U_\Lambda^{(\Xi)} \simeq 2U_\Xi^{(\Lambda)} \simeq 2U_\Lambda^{(\Lambda)}. \tag{8}$$

These relations were established based on one-boson exchange models and semi-empirical evaluation of the strength of the $\Lambda - \Lambda$ attraction (Schaffner et al. 1994).

Our aim is to adjust the parameters of our Lagrangian to reproduce, to within a few percent, ten semi-empirical nuclear and hyper-nuclear data. As we have mentioned in the introduction, the term "semi-empirical" refers to an indirect, model-dependent way of extracting these parameters from a wealth of experimental data. We first consider five nuclear matter parameters at saturation. The modern models used to extract the nuclear matter data are energy-density functionals of a sufficiently rich structure. Their parameters are adjusted to fit the masses and charge-radii (and often some additional data) of a broad sample (some thousands) of atomic nuclei. An extrapolation to the limiting case of infinite nuclear matter is then made, yielding *semi-empirical* values of n_s, E_s, K_s, S_s, and L. The scatter in the values of the nuclear-matter parameters extracted in this way visualizes the model dependence of the procedure used. In particular, systematic differences are noticed for K_s: non-relativistic models give typically 210–240 MeV, while the relativistic ones yield larger values 260–290 MeV. The starting point for our Lagrangian, Sect. 2, was a very successful relativistic model TM1 (Sugahara & Toki 1994), and therefore we kept its values of n_s, E_s, and K_s. Our results for the nuclear matter parameters at saturation are presented in Table 3.

Our adjustement of the isovector parameters in Lagrangian density, namely g_ρ and Λ_V, deserves additional explanation. We performed this by employing existing information on the density dependence of the symmetry energy, that is, we used not only the value of the symmetry energy at saturation, S_s, but also a semi-empirical estimate of symmetry energy at $n_\mathrm{b} \approx 0.1\ \mathrm{fm}^{-3}$, 26.67 MeV, which determined the value of L (Horowitz & Piekarewicz 2001). This influenced the EOS of neutron matter, because $E(n_\mathrm{b}, 1) \approx E(n_\mathrm{b}, 0.5) + S(n_\mathrm{b})$ (see, e.g., Haensel et al. 2007).

4. EOS of neutron-star matter

The total energy density and the total pressure are the sums of the contributions of hadrons and leptons, because the contributions of the electromagnetic interaction to these quantities are negligibly small, and leptons (electrons and muons) can be treated as ideal Fermi gases, such that

$$\mathcal{E} = \mathcal{E}_\mathrm{had} + \mathcal{E}_\mathrm{lep}, \quad P = P_\mathrm{had} + P_\mathrm{lep}. \tag{9}$$

The (total) baryon number density is

$$n_\mathrm{b} = \sum_B n_B. \tag{10}$$

Imposing electrical charge neutrality and beta equilibrium, one gets a system of non-linear equations for the particle species fractions $Y_\mathrm{i} = n_\mathrm{i}/n_\mathrm{b}$. At a given n_b the equilibrium fractions are $\{Y_\mathrm{i}^0(n_\mathrm{b})\}$ and the energy density and pressure become functions only of n_b. For the sake of comparison, we consider not only a general EOS involving nucleons and hyperons, EOS.NH, but also an EOS of nucleon matter, EOS.N, with artificially suppressed hyperons (see Sect. 1).

Expression for P_had, Eq. (3), shows that hyperons produce new repulsive quartic terms involving f_0, w_0, and r_0. The dependence of the EOS on Λ_V turns out to be quite strong. All other parameters are determined by the conditions of reproducing nuclear and hypernuclear data (i.e., near the saturation point of nuclear matter), and the high-density stiffness of EOS.NH increases monotonically with increasing Λ_V. In what follows, we use $\Lambda_\mathrm{V} = 0.0165$, which as we see yields a high-density stiffness of the EOS.NH consistent with $M_\mathrm{max}^\mathrm{(NH)} > 2\ M_\odot$, while keeping good agreement with semi-empirical nuclear matter parameters. This EOS.NH is referred to hereafter as BM165.

The parameters of the BM165 model, and the values of ten semi-empirical nuclear and hyper-nuclear parameters given by this model, are presented in Tables 1–4.

The thermodynamical equilibrium of the NH matter imposes relations between the chemical potentials of hyperons *present*

Table 1. BM165 model of hadronic matter.

m_σ (MeV)	$g_{N\sigma}$	$g_{\Lambda\sigma}$	$g_{\Sigma\sigma}$	$g_{\Xi\sigma}$	g_3 (fm^{-1})
511.198	10.0289	6.169	4.476	3.201	7.2325
$m_{\sigma^\star}$ (MeV)	$g_{N\sigma^\star}$	$g_{\Lambda\sigma^\star}$	$g_{\Sigma\sigma^\star}$	$g_{\Xi\sigma^\star}$	g_4
975.0	0	5.482	5.482	11.372	0.6183

Notes. Masses and coupling constants of scalar mesons. We neglect mass-splitting within charge multiplets of the baryon octet assuming that: $m_\mathrm{n} = m_\mathrm{p} = 938.919$ MeV, $m_\Lambda = 1115.63$ MeV, $m_\Sigma = 1193.12$ MeV, and $m_\Xi = 1318.1$ MeV.

Table 2. BM165 model of hadronic matter.

m_ω (MeV)	m_ρ (MeV)	m_ϕ (MeV)	$g_{N\omega}$	$g_{N\rho}$
783.0	770.0	1020.0	12.6139	10.037

Notes. We provide both the masses and coupling constants of the vector mesons. The coupling constants in the quartic terms are $c_3 = 71.3075$ and $\Lambda_\mathrm{V} = 0.0165$.

Table 3. BM165 model of hadronic matter.

n_s (fm^{-3})	E_s (MeV)	K_s (MeV)	S_s (MeV)	L (MeV)
0.145	–16.3	279	33	74

Notes. Calculated nuclear matter parameters at the saturation point.

Table 4. BM165 model of hadronic matter.

$U_N^{(N)}$ (MeV)	$U_\Lambda^{(N)}$ (MeV)	$U_\Sigma^{(N)}$ (MeV)	$U_\Xi^{(N)}$ (MeV)	$U_\Lambda^{(\Lambda)}$ (MeV)
–69	–28	+30	–18	–5

Notes. Calculated zero-momentum single-baryon potentials in symmetric nuclear matter, $U_B^{(\mathrm{N})}$ and of Λ in Λ matter, $U_\Lambda^{(\Lambda)}$. All results are obtained at $n_\mathrm{b} = n_\mathrm{s}$.

in dense matter, nucleons, and leptons. These relations can be expressed in the general form (see, e.g., Haensel et al. 2007)

$$\mu_{\rm H} = \mu_{\rm n} - q_{\rm H}\mu_{\rm e}, \quad \mu_{\rm e} = \mu_\mu, \tag{11}$$

where $q_{\rm H}$ is the charge of the hyperon H in units of the proton charge. The threshold density for the appearance of hyperons H, $n_{\rm b}^H$, is determined by the enthalpy of a single hyperon H in beta-equilibrated dense matter

$$\mu_{\rm H}^{(0)} = m_{\rm H} + U_{\rm H} + P/n_{\rm b}, \tag{12}$$

where $U_{\rm H}$ is the potential energy of this hyperon. For $n_{\rm b} < n_{\rm b}^H$, $\mu_{\rm H}^{(0)} > \mu_{\rm n} - q_{\rm H}\mu_{\rm e}$, and H decays in a weak interaction process. At the threshold density, a single H in dense matter is stable so that

$$\mu_{\rm H}^{(0)} = \mu_{\rm n} - q_{\rm H}\mu_{\rm e}, \tag{13}$$

and for $n_{\rm b} > n_{\rm b}^H$, the density of stable H grows with increasing $n_{\rm b}$.

For the BM165 model, the first hyperon to appear is Λ at 6.3×10^{14} g cm^{-3} (0.35 fm^{-3}), where $\mu_\Lambda^{(0)} = \mu_n$. The next hyperon is Ξ^-, which appears at 7.7×10^{14} g cm^{-3} (0.42 fm^{-3}), where $\mu_{\Xi^-}^{(0)} = \mu_n + \mu_e$. A repulsive $U_{\Sigma^-}^{(N)}$ implies that Σ^- appears at significantly higher density than Ξ^-, namely 1.23×10^{15} g cm^{-3} (0.63 fm^{-3}), even though $m_{\Sigma^-} < m_{\Xi^-}$.

The order of appearance of hyperons in dense matter deserves a comment. For a long time, in view of the lack of experimental information on $U_\Sigma^{(N)}$ and $U_\Xi^{(N)}$, they were assumed to be similar to $U_\Lambda^{(N)}$. Consequently, Σ^- was found to be the first hyperon to appear, not the lightest hyperon Λ, because the (unfavorable) effect of $m_{\Sigma^-} > m_\Lambda$ was weaker than the (favorable) effect of the presence of $\mu_{\rm e}$ in the threshold condition $\mu_{\Sigma^-}^{(0)} = \mu_{\rm n} + \mu_{\rm e}$ (see, e.g., Haensel et al. 2007). However, the large positive (repulsive) $U_\Sigma^{(N)}$ derived by analyses of the Σ^--atoms pushes $n_{\rm b}^{\Sigma^-}$ well above $n_{\rm b}^{\Xi^-}$. Consequently, Σ^- is the last, instead of the first, hyperon to appear in a neutron star core (Fig. 2).

The appearance of hyperons leads to significant softening of the EOS.NH compared to EOS.N (Fig. 1). To be able to model neutron stars with $M > 2\ M_\odot$, the EOS.NH has *necessarily* to significantly *stiffen* at higher densities. The curve $P^{\rm NH}(\rho)$ crosses the $P^{\rm N}(\rho)$ one at $\rho_2 = 1.76 \times 10^{14}$ g cm^{-3} ($n_2 = 0.85$ fm^{-3}), and at higher density the EOS.NH is stiffer than the EOS.N.

In reality, the difference $P^{\rm NH} - P^{\rm N}$ is limited by the stability of the NH phase against the re-conversion into the N phase. We assume that the matter is in beta equilibrium. At T = 0, the small change in energy per baryon dE is related to the small change in the baryon density d$n_{\rm b}$ by

$$\mathrm{d}E = P\frac{\mathrm{d}n_{\rm b}}{n_{\rm b}^2}. \tag{14}$$

Therefore, the condition for the stability of the NH phase (against the conversion into the N one)

$$E^{\rm NH}(n_{\rm b}) < E^{\rm N}(n_{\rm b}), \tag{15}$$

implies that

$$\int_{n_1}^{n_{\rm b}} \frac{P^{\rm NH}(n'_{\rm b}) - P^{\rm N}(n'_{\rm b})}{{n'_{\rm b}}^2}\mathrm{d}n'_{\rm b} < 0, \tag{16}$$

where n_1 is the density at the first hyperon threshold. For the BM165 model, $n_1 = 0.35$ fm^{-3}.

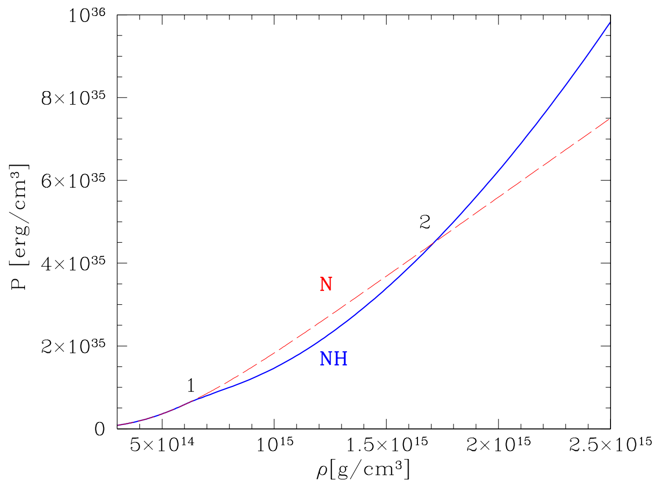

Fig. 1. Equations of state EOS.N and EOS.NH calculated using the BM165 model. Hyperons appear at point 1 and the EOS.NH crosses the EOS.N one at point 2.

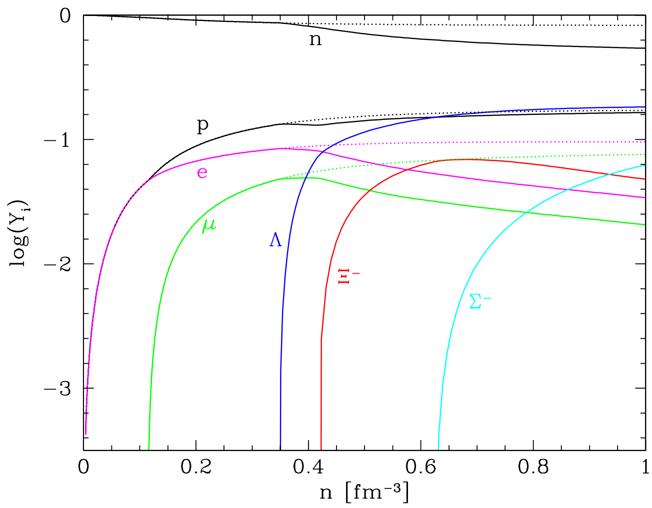

Fig. 2. Number fractions of the constituents of dense matter in beta equilibrium, $Y_{\rm i} = n_{\rm i}/n_{\rm b}$, versus baryon density, $n_{\rm b}$. Dotted lines: EOS.N. Solid lines: EOS.NH.

5. A model of PSR J1614-2230

To get a complete EOS of the neutron-star interior, the BM165 EOS of the liquid core was supplemented by an EOS of the crust. We used the EOS of the inner crust of Douchin & Haensel (2001), the model of Haensel & Pichon (1994) for the outer crust down to 10^8 g cm^{-3}, and the classical model of Baym et al. (1971) for the outer layer with $\rho < 10^8$ g cm^{-3}. A model of a neutron star of gravitational mass 1.97 $M_\odot$, rotating rigidly at 317 Hz, was calculated using the two-dimensional `rotstar` code from the LORENE library[1] implementing the formulation of Bonazzola et al. (1993). The circumferential equatorial radius of neutron star is $R_{\rm eq} = 11.83$ km, its central density $\rho_{\rm c} = 1.73 \times 10^{14}$ g cm^{-3}, and its central baryon density $n_{\rm c} = 0.834$ fm^{-3}. At 317 Hz, polar flattening is rather small: the radial coordinate at the equator is only 200 m larger than that at the pole. The number fractions of the particle species $Y_{\rm i} = n_{\rm i}/n_{\rm b}$ in the liquid core of neutron star, are plotted versus the radial coordinate r in Fig. 4. The radius of the hyperon

[1] http://www.lorene.obspm.fr

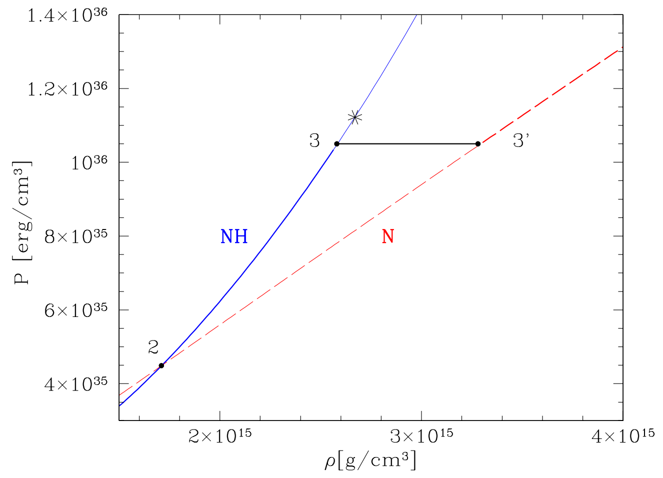

Fig. 3. EOS BM165 in the vicinity of the high-density NH-N phase transition, where 2 is the crossing of the the N and NH pressures, 3 represents the density and pressure of the NH phase at the phase coexistence, and 3′ is the density and pressure of the N phase at the phase coexistence. Horizontal segment 33′ is the pressure at the first order phase transition. Were the NH phase to be (sufficiently) stable until reaching a maximum mass, maximum (central) density in stable stars would correspond to the asterisk sign, $\rho_{\rm c,max} = \rho_*$. For the fully equilibrated hadronic matter $\rho_{\rm c,max}$ is slightly higher than ρ'_3. For a more detailed discussion of this point, see the text.

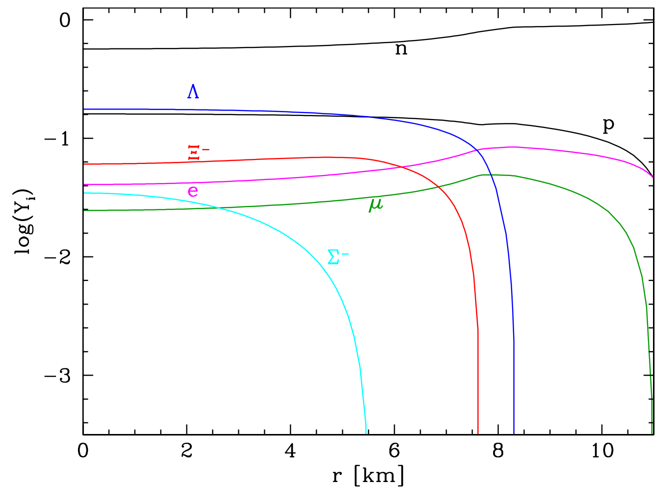

Fig. 4. The logarithm of the number fractions of the constituents of dense matter, $\log_{10}(Y_{\rm i})$, versus circumferential radius, in the liquid core of a 1.97 $M_\odot$ star model based on the BM165 EOS.

core is 8.36 km. The strangeness per baryon at the star's center is $(S/N_{\rm b}) = -0.35$.

6. High-density instability of the NH phase and neutron star models

Violation of the inequality (16) indicates that the NH phase is unstable with respect to a conversion into a purely nucleon (N) one. Thermodynamic equilibrium of dense matter at pressure P corresponds to the minimum of the baryon chemical potential $\mu_{\rm b} = (\mathcal{E} + P)/n_{\rm b}$. An equilibrium phase-transition NH⟶N occurs at P_3 such that

$$\mu_{\rm b}^{\rm (NH)}(P_3) = \mu_{\rm b}^{\rm (N)}(P_3), \tag{17}$$

and is accompanied by a density jump from $\rho_3 = \rho^{\rm (NH)}(P_3) = 2.58 \times 10^{15}$ g cm^{-3} ($n_3 = 1.105$ fm^{-3}) on the NH side to $\rho'_3 = \rho^{\rm (N)}(P_3) = 3.25 \times 10^{15}$ g cm^{-3} ($n'_3 = 1.31$ fm^{-3}) on the N side. The BM165 EOS in the vicinity of $P_3 = 1.05 \times 10^{36}$ erg cm^{-3} is shown in Fig. 3. The softening of the EOS for $P > P_3$ is twofold. First, there is a constant pressure sector of the EOS (corresponding to the vanishing compression modulus!). Second, there is a transition to the N-phase, which is significantly softer than the NH one.

The reaction of the stellar structure to the (first order) phase transition (NH⟶N) can be described by the linear response theory formulated in Zdunik et al. (1987). This theory describes stellar configurations in the vicinity of a star that has a central pressure equal to P_3. In our case, this region of stellar configurations is very small because we are close to the maximum mass. The crucial parameter, determining the stability of the star with a small core of the denser phase (N), is the relative density jump at phase transition pressure, P_3 of $\lambda = \rho'_3/\rho_3$. The stability condition for a star with a small N-core is

$$\lambda < \lambda_{\rm crit} = \frac{3}{2}\left(1 + \frac{P_3}{\rho_3 c^2}\right) \tag{18}$$

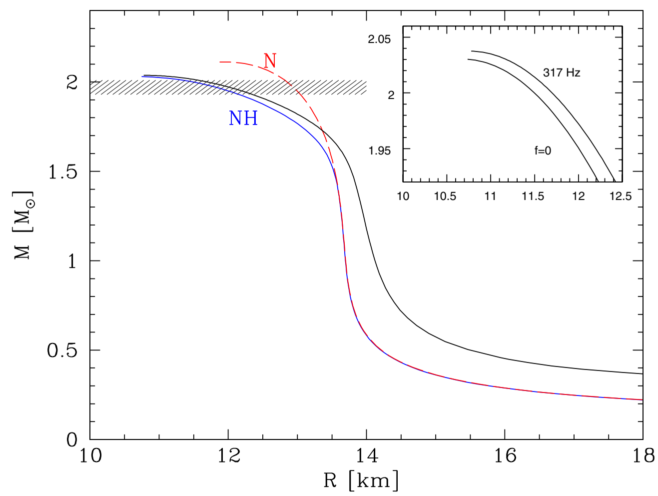

Fig. 5. Gravitational stellar mass, M, versus circumferential radius, R, calculated for the EOS.N and EOS.NH. Only stable configurations are displayed. Inset: effect of rotation at $f = 317$ Hz on the M – equatorial circumferential radius curve near $M_{\rm max}$.

(see Sect. 3.4 of Zdunik et al. 1987). In our case, the condition in Eq. (18) is fulfilled, because $\lambda = 1.27$ while $\lambda_{\rm crit} = 2.18$. Consequently, there is a (very small) region of stable configurations with the N-phase core. In reality, this region is very narrow: the maximum mass of non-rotating stars is reached for a central pressure $P_{\rm c,max}$ that is only higher by 0.04% than the pressure at the phase transition, P_3.

We plot in Fig. 5 the $M - R$ relations for non-rotating neutron stars, and those rotating at 317 Hz, based on the BM165 EOS. Stars with $M > 1.4\ M_\odot$ have a hyperon core. The flattening of the $M(R)$ curve due to the hyperon softening of the EOS is significant. However, it remains possible to achieve $M_{\rm max}^{\rm (NH)stat} = 2.03\ M_\odot$, which is smaller than $M_{\rm max}^{\rm (N)stat}$ by only 0.07 $M_\odot$. Rotation at 317 Hz, as measured for PSR J1614-2230, increases $M_{\rm max}^{\rm (NH)}$ to 2.04 $M_\odot$ (see zoomed inset of Fig. 5).

7. Discussion and conclusions

We have constructed a model of the hyperon cores of neutron stars that allows for the existence of neutron star of 2 $M_\odot$.

The model is consistent with ten semi-empirical evaluations of nuclear and hyper-nuclear matter parameters. As an additional constraint, we have imposed SU(6) symmetry relations between the coupling constants of baryons and vector mesons. In spite of this, by introducing two hidden-strangeness meson fields (scalar and vector) coupled only to hyperons, we have been able to reproduce four semi-empirical parameters stemming from hypernuclear physics.

In contrast to the NL3 model, which was used by Bonanno & Sedrakian (2012), our symmetry energy is not unusually "stiff" near the saturation point: we get $L = 74$ MeV, compared to $L = 118$ MeV for NL3 (Agrawal et al. 2005). Consistently, our EOS.N is not unusually stiff, and yields for NS with nucleon cores $M_{\rm max}^{\rm (N)stat} = 2.10\ M_\odot$, which to be contrasted with the NL3 value of 2.8 $M_\odot$. The hyperon softening for the model of Bonanno & Sedrakian (2012) is dramatic, and leads to $M_{\rm max}^{\rm (NH)stat}$, which is lower by nearly 0.8 $M_\odot$ than the N one. In our case, getting $M_{\rm max}^{\rm (NH)stat} > 2.0\ M_\odot$ is conditioned by the high-density vector interactions in the hyperon sector, which are not excluded in view of our lack of knowledge of high-density hyperon interactions. A similar solution was proposed Weissenborn et al. (2012b,a), who obtained the stiffening of the EOS.NH from the ϕ meson coupled to hyperons.

Our EOS.NH becomes stiffer than the EOS.N for $\rho \gtrsim 5\rho_0$, and its stiffness grows with density. This leads eventually to the instability of the NH matter with respect to the conversion into the N state, softening the EOS due to the first order phase transition. The maximum density at which the stable NH phase can exist actually determines our $M_{\rm max}^{\rm (NH)stat}$, which is only 0.07 $M_\odot$ lower than $M_{\rm max}^{\rm (N)stat}$. The rotation at 317 Hz, as measured for PSR J1614-2230, increases $M_{\rm max}^{\rm (NH)}$ by 0.01 $M_\odot$, to 2.04 $M_\odot$. Breaking the SU(6) symmetry for the vector-meson couplings to hyperons, in a similar way to Weissenborn et al. (2012a), can make the value of $M_{\rm max}^{\rm (NH)}$ even higher.

In the present paper, we have restricted ourselves to the hadronic forms of matter. A consistent treatment of the phase transition to the quark phase in the neutron star core would require the use of the QCD for both hadronic and quark phases. As the transition occurs in the strong-coupling regime, one is forced to use different models that separately describe the baryon and the quark phases. An approach based on an effective model of the QCD of quark matter (Nambu-Jona-Lasinio) and NL3 for the hadronic phase, used by Bonanno & Sedrakian (2012) indicates that to get $M_{\rm max} > 2\ M_\odot$, vector repulsion in quark matter should be sufficiently strong. In any case, the maximum mass obtained by them is very close to that reached at a central density equal to the deconfinement density.

Acknowledgements. We are deeply grateful to Mikhail E. Gusakov for his invaluable help in detecting and removing some errors in earlier versions of the present work. We are also indebted to him for his difficult but inspiring questions referring to the physics of dense matter. We are grateful to Verônica Antocheviz Dexheimer for pointing out one of the missing references. This work was partially supported by the Polish MNiSW research grant no. N N203 512838, by the LEA Astro-PF, and by the European Science Foundation CompStar RNP. MB acknowledges the support of Marie Curie Fellowship no. ERG-2007-224793 within the 7th European Community Framework Programme.

References

Agrawal, B. K., Shlomo, S., & Kim Au, V. 2005, EpJ A, 25, 525
Akmal, A., Pandharipande, V. R., & Ravenhall, D. G. 1998, Phys. Rev. C, 58, 1804
Baym, G., Pethick, C., & Sutherland, P. 1971, ApJ, 170, 299
Bednarek, I., & Manka, R. 2009, J. Phys. G Nucl. Phys., 36, 095201
Bombaci, I., Panda, P. K., Providencia, C., & Vidana, I. 2008, Phys. Rev. D, 77, 083002
Bonanno, L., & Sedrakian, A. 2012, A&A, 539, A16
Bonazzola, S., Gourgoulhon, E., Salgado, M., & Marck, J.-A. 1993, A&A, 278, 421
Burgio, G. F., Schulze, H.-J., & Li, A. 2011, Phys. Rev. C, 83, 025804
Champion, D. J., Ransom, S. M., Lazarus, P., et al. 2008, Science, 320, 1309
Chatterjee, D., & Schaeffner-Bielich, J. 2011, Poster presented at CompStar2011 Workshop, Catania, Italy
Demorest, P. B., Pennucci, T., Ransom, S. M., Roberts, M. S. E., & Hessels, J. W. T. 2010, Nature, 467, 1081
Dexheimer, V., & Schramm, S. 2008, ApJ, 683, 943
Douchin, F., & Haensel, P. 2001, A&A, 380, 151
Endo, T., Maruyama, T., Chiba, S., & Tatsumi, T. 2006, Prog. Theor. Phys., 115, 337
Freire, P. C., Bassa, C. G., Wex, N., et al. 2011, MNRAS, 412, 2763
Glendenning, N. K. 1985, ApJ, 293, 470
Glendenning, N. K. 1996, Compact Stars. Nuclear Physics, Particle Physics, and General Relativity (New York: Springer)
Glendenning, N. K., & Moszkowski, S. A. 1991, Phys. Rev. Lett., 67, 2414
Haensel, P., & Pichon, B. 1994, A&A, 283, 313
Haensel, P., Potekhin, A. Y., & Yakovlev, D. G. 2007, Neutron Stars 1. Equation of State and Structure (New York: Springer)
Horowitz, C. J., & Piekarewicz, J. 2001, Phys. Rev. Lett., 86, 5647
Schaffner, J., Dover, C. B., Gal, A., et al. 1994, Ann. Phys. (NY), 235, 35
Schaffner-Bielich, J., & Gal, A. 2000, Phys. Rev. C, 62, 034311
Song, H. Q., Su, R. K., Lu, D. H., & Qian, W. L. 2003, Phys. Rev. C, 68, 055201
Sugahara, Y., & Toki, H. 1994, Nucl. Phys. A, 579, 557
Takahashi, H., Ahn, J. K., Akikawa, H., et al. 2001, Phys. Rev. Lett., 87, 212502
Vidana, I., Logoteta, D., Providencia, C., & Bombaci, I. 2011, Europhys. Lett., 94, 11002
Walecka, J. D. 2004, Theoret. Nucl. Subnucl. Phys., 2nd ed. (World Scientific: Imperial College Press)
Weissenborn, S., Chatterjee, D., & Schaffner-Bielich, J. 2012a, Phys. Rev. C, 85, 065802
Weissenborn, S., Chatterjee, D., & Schaffner-Bielich, J. 2012b, Nucl. Phys. A, 881, 62
Zdunik, J. L., Haensel, P., & Schaeffer, R. 1987, A&A, 172, 95